Stochastic Simulation for Morphological Development During the Isothermal Crystallization of Semicrystalline Polymers: A Case Study of Syndiotactic Polypropylene

Siripon Anantawaraskul,[1] Saraporn Ketdee,[1] Pitt Supaphol[2]

[1]*Department of Chemical Engineering, Kasetsart University, 50 Phaholyothin Road, Jatujak, Bangkok 10900, Thailand*
[2]*Petroleum and Petrochemical College, Chulalongkorn University, Soi Chula 12, Phyathai Road, Pathumwan, Bangkok 10330, Thailand*

Received 25 December 2007; accepted 14 August 2008
DOI 10.1002/app.29230
Published online 13 November 2008 in Wiley InterScience (www.interscience.wiley.com).

ABSTRACT: A stochastic simulation scheme for predicting morphological development during nucleation and subsequent crystal growth based on predetermined crystallization kinetic data of a semicrystalline polymer under quiescent isothermal conditions is proposed. Based on previously obtained crystallization kinetic data for syndiotactic polypropylene (s-PP) used as the input information, the simulation scheme was successful in predicting the morphological development of s-PP during isothermal crystallization from the melt state. The predicted development of crystallinity during crystallization was reanalyzed with the Avrami macrokinetic model, and good agreement between the predicted and theoretical values for s-PP was observed. On the basis of this simulation scheme, both the spherulite size and its distribution during the course of crystallization could also be predicted. Although the spherulitic growth rate influenced both the spherulite size and its distribution during the course of crystallization, it had no effect on the final spherulitic morphology or the resulting average spherulitic size. © 2008 Wiley Periodicals, Inc. J Appl Polym Sci 111: 2260–2268, 2009

Key words: crystallization; Monte Carlo simulation; morphology; poly(propylene) (PP)

INTRODUCTION

The crystallization of semicrystalline polymers is a major research interest in the field of polymer physics that has implications for engineering as well because a quantitative understanding of this issue and related phenomena could lead to predictive control over the properties (e.g., physical, mechanical, and optical properties) of the finished products.[1] From an engineering point of view, two key domains of interest in polymer crystallization are the crystallization kinetics, which provide information on the time dependence of the developed crystallinity, and the crystalline morphology, which is a mesoscale structure directly influencing the properties of the polymers.

Polymer crystallization consists of two important processes: nucleation and crystal growth. In the nucleation process, nuclei of a critical size are formed when the thermodynamic condition is satisfied.[2] The critical size and number of nuclei are controlled mainly by crystallization conditions (e.g., temperature and pressure). The formed nuclei act as seeds for crystallites to grow during the subsequent crystal growth. Generally, for each polymer, the rate of crystal growth is a function of the crystallization temperature (T_c) and can be considered a constant when the crystallization is considered under an isothermal condition. For highly crystalline polymers, each crystallite can grow until it impinges on adjacent crystallites and its growth abruptly stops at the formed boundary. Both nucleation and growth processes are known to influence crystallization kinetics and the final morphology.

Numerous studies on crystallization kinetics and crystalline morphology have been conducted with several experimental techniques.[3,4] Differential scanning calorimetry (DSC) can effectively provide quantitative information on the overall crystallization kinetics. Polarized light microscopy and atomic force microscopy can provide quantitative information on the nucleation rate and growth rate but only qualitative information on the morphology in detail (i.e., the average crystallite size and crystallite size distribution). Therefore, our understanding of the relationship between the morphology and properties is largely qualitative (e.g., a polymer with a large crystallite size will be more brittle than a polymer with a small crystallite size). From an engineering point of

Correspondence to: S. Anantawaraskul (fengsia@ku.ac.th).
Contract grant sponsor: National Center of Excellence for Petroleum, Petrochemicals, and Advanced Materials of Thailand.

view, a more quantitative understanding of such a relationship is necessary to realize better control over the properties of a semicrystalline polymer.

Recently, a new methodology for predicting the final morphology and overall crystallization kinetics of a semicrystalline polymer based on a stochastic simulation[5–10] and a phase-field model[11,12] has been proposed. This computational approach allows for a separate examination of the effect of each parameter governing the crystallization process (e.g., the number of nuclei and growth rate), which is hard to realize experimentally as several parameters change simultaneously. Furthermore, this approach can also provide quantitative information on the morphological development in detail, which is difficult to achieve experimentally. This gives an edge to the computational approach that can provide useful information for better process control during polymer processing.

In previous reports, most researchers mainly focused on the effects of crystallization parameters on the crystallization kinetics and final morphology, but no one has investigated the morphological development during crystallization in detail. Recently, we developed an algorithm to investigate the influence of both nucleation and growth processes on the morphological development and crystallization kinetics in detail.[13] In this work, we further implement this stochastic simulation to probe the effect of T_c on both morphological development (e.g., the crystallinity, average crystallite size, and crystallite size distribution as a function of time) and overall crystallization kinetics during the isothermal crystallization of syndiotactic polypropylene (s-PP), which is used as the model system, on the basis of our previously published data.[14,15]

The quantitative understanding of morphological development obtained from this work is envisioned as a stepping stone to the future development of an algorithm that gives details about processing–morphology–property interrelationships. As the crystalline morphology of a semicrystalline polymer can be controlled to some degrees by operating conditions (e.g., the temperature, pressure, and shear stress), these relationships will allow us to fine-tune the final properties though appropriate control over the operating conditions.

THEORETICAL BACKGROUND AND RELATED EXPERIMENTAL WORKS

The Avrami macrokinetic model is an equation theoretically derived for describing the overall crystallization kinetics (i.e., the crystallinity evolution) under isothermal conditions.[16,17] In the Avrami macrokinetic model, the developed crystallinity [$\theta(t)$] can be written as a function of the crystallization time (t) as follows:

$$\theta(t) = 1 - \exp[-k_a t^{n_a}] \in [0,1] \quad (1)$$

where k_a and n_a are the Avrami crystallization rate constant and the Avrami exponent, respectively. For a given crystallization condition, both k_a and n_a are constants. For simplicity, heterogeneous nucleation and spherulitic morphology were assumed in our study. On the basis of this assumption, the parameter k_a is related to the total concentration of the predetermined nuclei (N_{tot}) and the spherulitic growth rate (G) according to the following equation[3]:

$$k_a = \pi N_{\text{tot}} G^2 \quad (2)$$

For the purpose of our study, the Avrami macrokinetic model is used to validate the applicability of our algorithm by a comparison of the results obtained from the model prediction with those reported in the literature.[14,15]

To investigate the kinetics of G for a semicrystalline polymer under isothermal conditions, the secondary nucleation theory proposed by Lauritzen and Hoffman is often used.[15] Based on this proposition, G is related to T_c according to an exponential equation of the following form:

$$G = G_0 \exp\left[-\frac{U^*}{R(T_c - T_\infty)}\right] \exp\left[-\frac{K_g}{T_c(\Delta T)f}\right] \quad (3)$$

where G_0 is a temperature-independent pre-exponential factor, U^* is the activation energy for the transportation of segments of molecules across the melt/solid surface boundary (usually given as a value of 1500 cal/mol),[9,10,14–16,18] T_∞ signifies the cessation of long-range molecular motion (i.e., $T_\infty = T_g - 30$, where T_g is the glass-transition temperature), R is the universal gas constant, ΔT is the degree of undercooling (i.e., $\Delta T = T_m^0 - T_c$, where T_m^0 is the equilibrium melting temperature), f is a correction factor for the temperature dependence of the enthalpy of fusion [i.e., $f = 2T_c/(T_c + T_m^0)$], and K_g is the nucleation exponent. Practically, the temperature dependence of k_a can be described by an equation similar to that of eq. (3)[15]:

$$\Psi(T_c) = \Psi_0 \exp\left[-\frac{\Theta}{R(T_c - T_\infty)}\right] \exp\left[-\frac{K^G}{T_c(\Delta T)f}\right] \quad (4)$$

where $\Psi(T_c)$ and Ψ_0 are the overall crystallization rate parameter (e.g., k_a) and the pre-exponential parameter (e.g., k_{a0}), respectively; Θ is a parameter related to the activation energy characterizing the molecular transport across the melt/solid interface; and K^G is a combined factor related to the secondary nucleation mechanism.

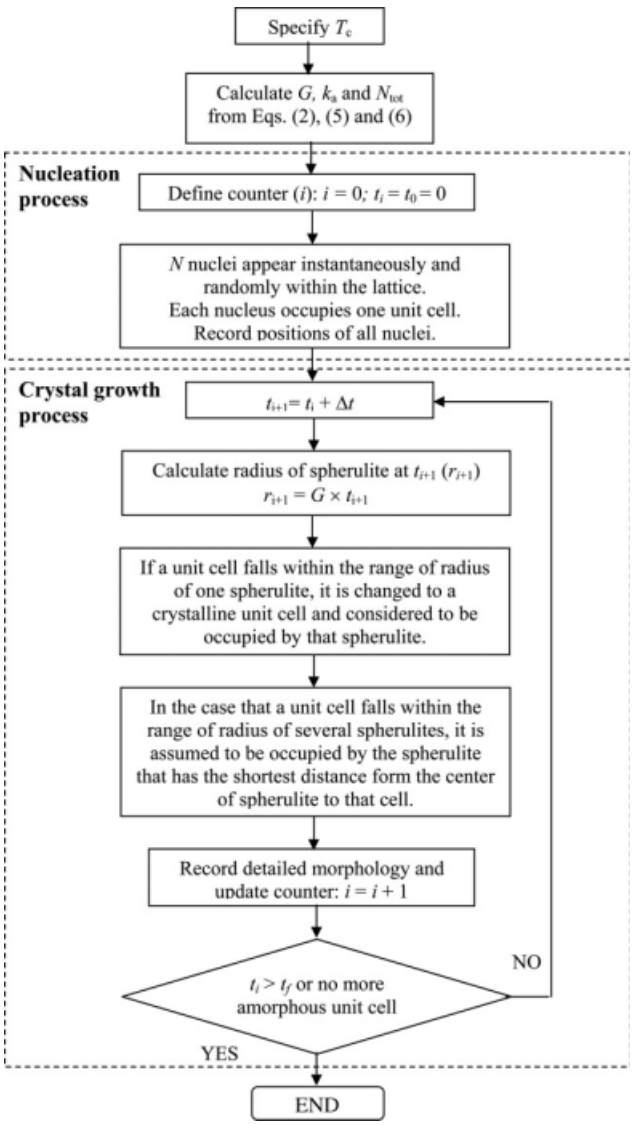

Figure 1 Simplified algorithm for the stochastic simulation scheme.

Recently, the isothermal melt-crystallization kinetics of s-PP was investigated with DSC.[15] The overall crystallization kinetics was determined by the direct fitting of the experimental data to the Avrami model. The temperature dependence of k_a was described by eq. (4) over the T_c range of 40–90°C:

$$k_a = 7.08 \times 10^{26} \exp\left[-\frac{1807.1}{T_c - 237}\right] \times \exp\left[-\frac{1.39 \times 10^6}{T_c(441.8 - T_c)f}\right] \quad (5)$$

where k_a has a unit of min^{-n} and f is equal to $2T_c/(T_c + 441.8)$. Note that the T_g and T_m^0 values for s-PP are −6 and 168.7°C, respectively. In addition, the isothermal spherulitic growth kinetics of s-PP was reported previously.[14] Here, the G function for regime III (over the T_c range of 45–110°C) was use to approximate the temperature dependence of G over the whole T_c range investigated:

$$G = 9.1 \times 10^8 \exp\left[-\frac{754.8}{T_c - 237}\right] \exp\left[-\frac{3.6 \times 10^5}{T_c(441.8 - T_c)f}\right] \quad (6)$$

where G has a unit of μm/min and f is equal to $2T_c/(T_c + 441.8)$.

For the purpose of this study, the nucleation mechanism was assumed to be heterogeneous in nature, and the spherulitic growth was two-dimensional. N_{tot} for a given T_c value could then be calculated from eqs. (2), (5), and (6). The values of N_{tot} and G for different T_c values were then used as input values in the stochastic simulation for the morphological development of spherulites in a two-dimensional space, from which the kinetics of the space filling was, in turn, used to arrive at the overall crystallization kinetics based on the Avrami macrokinetic proposition [i.e., eq. (1)].

STOCHASTIC SIMULATION OF MORPHOLOGICAL DEVELOPMENT AND OVERALL CRYSTALLIZATION KINETICS

Figure 1 shows the simplified algorithm used for our stochastic simulation. In the algorithm, we consider the graphical simulation of the crystallization process in a two-dimensional space (i.e., a square lattice with an active area of 800 × 800 unit cells). Each unit cell equals the real space of 0.04 μm^2 (i.e., 1 μm^2 = 25 unit cells). Initially, all 640,000 unit cells are considered an amorphous entity before the crystallization occurs. N_{tot} and G for a given T_c value in the range of 40–90°C were calculated from eqs. (2), (5), and (6), as previously mentioned. Table I summarizes the input data for this simulation.

At the onset of crystallization ($t = t_0 = 0$), the heterogeneous nucleation process occurs. The calculated number of nuclei (N) appears instantaneously and randomly within a square lattice. Each nucleus is

TABLE I
Values of the Input Parameters Used in the Simulation Scheme

Run	T_c (°C)	G (μm/min)	N_{tot} (nuclei/μm^2)	k_a (min^{-n})
Tc_40	40	0.93	0.0108	0.0294
Tc_45	45	1.47	0.0102	0.0696
Tc_50	50	2.11	0.0090	0.1257
Tc_55	55	2.76	0.0074	0.1768
Tc_60	60	3.34	0.0056	0.1954
Tc_65	65	3.74	0.0039	0.1704
Tc_70	70	3.88	0.0025	0.1167
Tc_75	75	3.72	0.0014	0.0622
Tc_80	80	3.30	0.0007	0.0254
Tc_85	85	2.68	0.0003	0.0077
Tc_90	90	1.99	0.0001	0.0017

The parameters $\Delta t = 2$, $t_0 = 0$, and $t_f = 100$ were held constant for all runs.

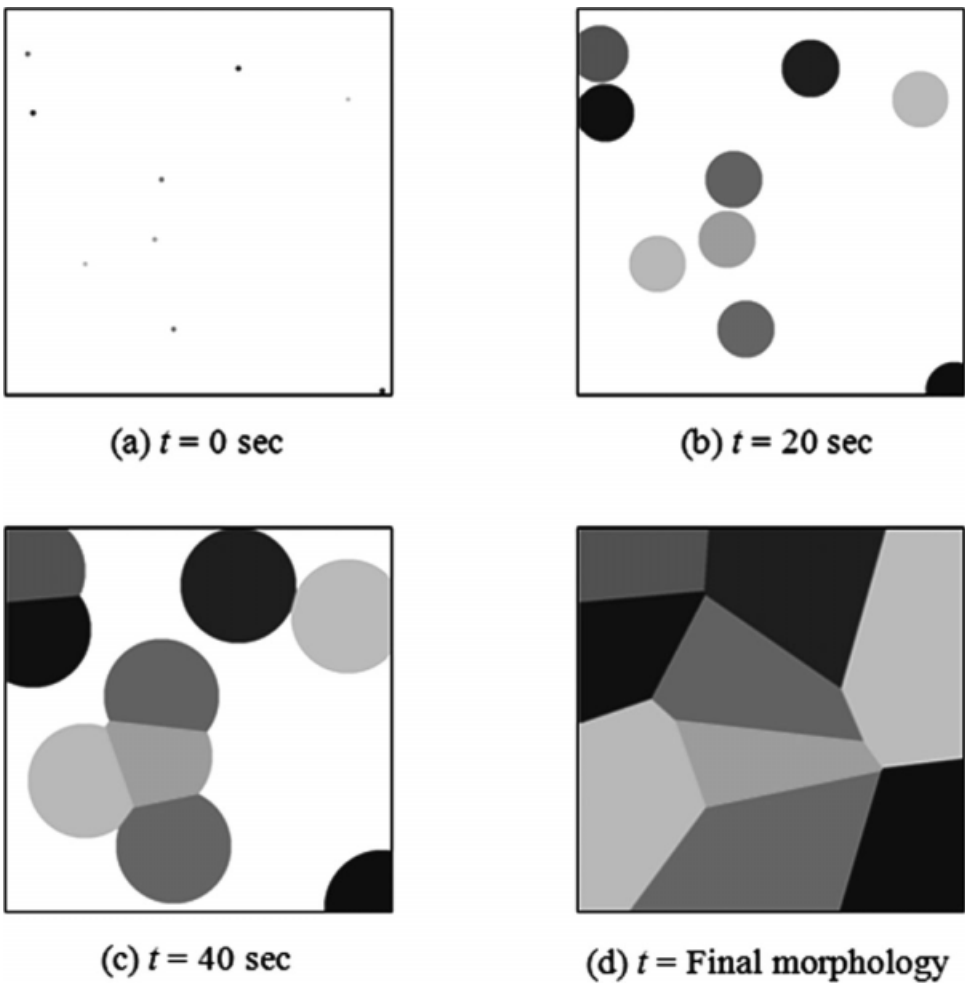

Figure 2 Examples of spherulitic morphology obtained from the simulation scheme at $T_c = 85°C$: (a) $t = 0$ s, (b) $t = 20$ s, (c) $t = 40$ s, and (d) final morphology.

assumed to occupy one unit cell, and the occupied unit cell changes from an amorphous entity to a crystalline one. The position of each nucleus is recorded by the program. After the nucleation process, t increases with a time step of Δt for each iteration (i.e., $t_{i+1} = t_i + \Delta t$; where the subscript indicates step time) until reaching the specified final time (t_f) or the complete crystallization. During the crystal growth, radius r of each spherulite can be computed from the product of G (unit cell/time step) and t; that is, $r = G \times t$. If an amorphous unit cell falls within the range of radius r of spherulite j, it is changed into a crystalline unit cell and considered to be occupied by spherulite j. In the case that

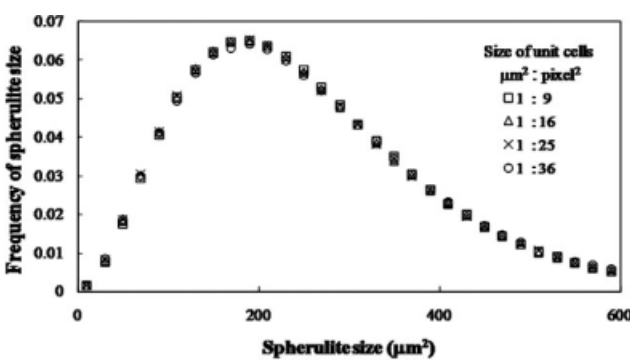

Figure 3 Effect of the unit cell size on the spherulite size distribution at the final morphology for $T_c = 65°C$.

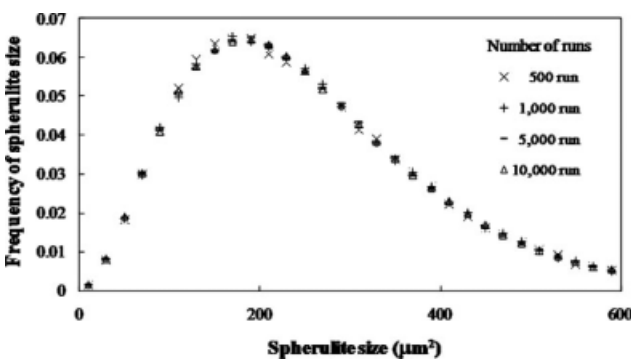

Figure 4 Effect of the number of runs on the spherulite size distribution at the final morphology for $T_c = 65°C$.

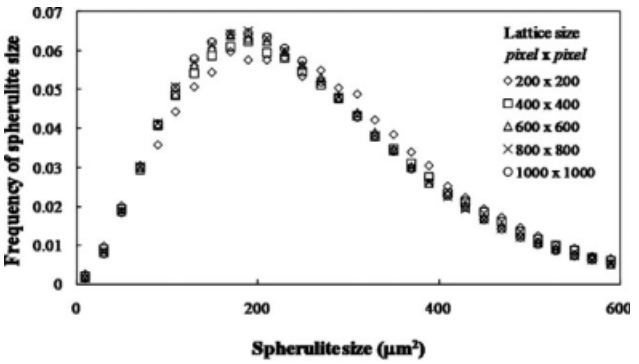

Figure 5 Effect of the lattice size on the spherulite size distribution at the final morphology for $T_c = 65°C$.

an amorphous unit cell falls within the range of radius r of several spherulites, it is assumed to be occupied by the spherulite that has the shortest distance from the center of the spherulite to that cell.

The morphology in detail (i.e., the crystallinity, average spherulite size, and spherulite size distribution) was recorded at each crystallization time. In the program, the crystallinity is defined as the ratio of the total number of crystalline unit cells (or occupied cells) to the total number of unit cells (i.e., 640,000). The average spherulite size can be calculated from the total number of crystalline unit cells divided by the total number of spherulites. This procedure is repeated until the specified t_f value or complete crystallization (i.e., no amorphous unit cell is available for further growth). Figure 2 illustrates morphological development obtained from the program at the T_c value of 85°C. Figure 2(a) shows the crystalline morphology at $t = 0$ s when heterogeneous nucleation occurs. Each spherulite grows individually without impingement during the first 20 s [i.e., Fig. 2(b)]. Several impingement boundaries occur as the crystallization time increases to 40 s [see Fig. 2(c)], and finally, the final spherulitic morphology is observed [see Fig. 2(d)].

As the positions of nuclei are chosen randomly for each run, a simulation using the same set of input data will generate different results for different runs.

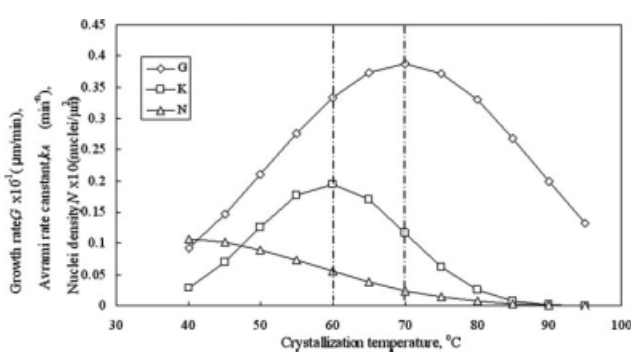

Figure 6 Effect of T_c on G, N_{tot}, and k_a.

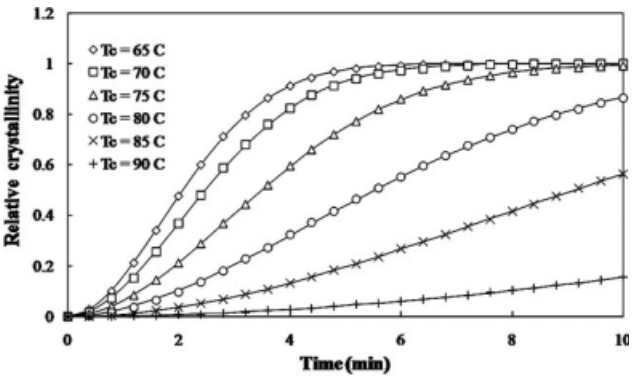

Figure 7 Effect of T_c (i.e., $T_c \in [65°C, 90°C]$) on the overall crystallization kinetics. Symbols show the predicted results from the simulation, and lines show the predictions according to the Avrami macrokinetic model.

By performing dependence tests on the size of each unit cell, the number of runs, and the lattice sizes (see Figs. 3–5), we found that the size of the unit cell is sufficiently small that it does not affect the simulated results. The average data from 5000 runs are adequate to obtain reliable information on morphological development and overall crystallization kinetics. The lattice size of 800 × 800 unit cells used in this work was sufficient for obtaining reliable results because the effect of the lattice boundary becomes negligible.

RESULTS AND DISCUSSION

Figure 6 shows G, N_{tot}, and k_a as functions of T_c for s-PP; they were calculated with eqs. (2), (5), and (6). G exhibits the typical bell-shaped dependence with T_c, and the maximum growth rate occurs at 70°C. This signifies the typical mobility-controlled mechanism at $T < T_c$ and the typical surface-nucleation-controlled mechanism at $T > T_c$. On the other hand, N_{tot} exhibits the expected monotonous increase with decreasing T_c. Clearly, k_a, signifying the overall

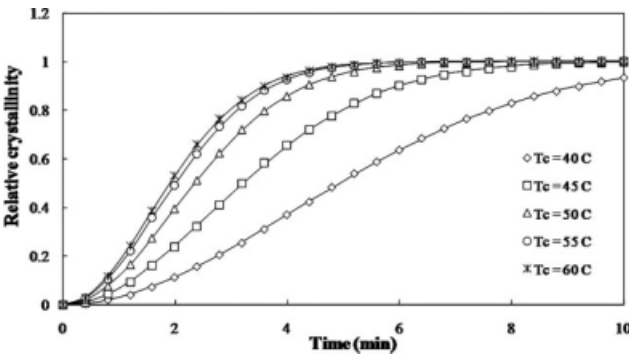

Figure 8 Effect of T_c (i.e., $T_c \in [40°C, 60°C]$) on the overall crystallization kinetics. Symbols show the predicted results from the simulation, and lines show the predictions according to the Avrami macrokinetic model.

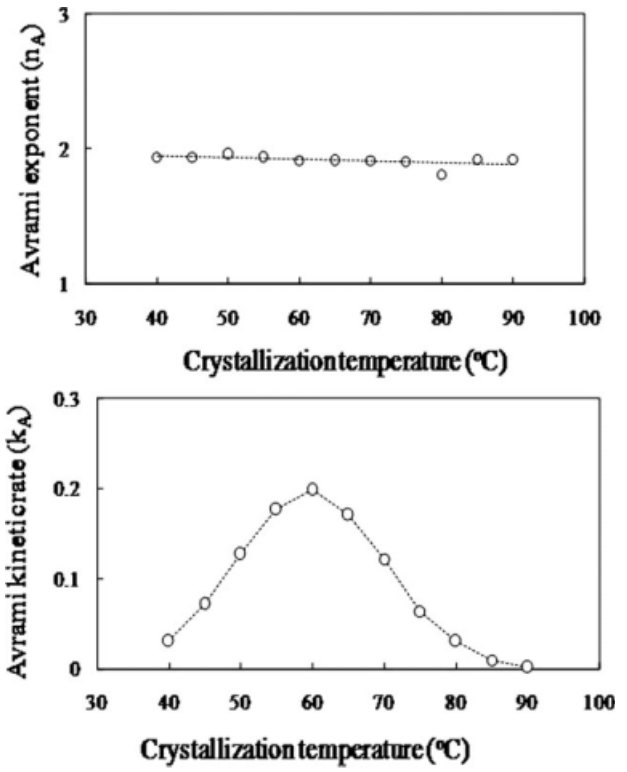

Figure 9 Avrami parameters obtained from the analysis of the simulated results based on the Avrami macrokinetic model. Lines are provided only to guide the eye.

crystallization rate, exhibits a temperature dependence on T_c similar to that of G, with the maximum being observed at 60°C.

Clearly, changes in T_c influence both N_{tot} and G simultaneously. As shown in Figure 6, when T_c decreases from 90 to 70°C, all the microscopic kinetic parameters, that is, G and N_{tot}, increase monotonically. This also results in a monotonic increase in k_a. When T_c decreases further from 70 to 60°C, despite the observed decrease in G, the observed increase in N_{tot} causes k_a to still increase. With a decrease in T_c from 60 to 40°C, G continues to decrease at a much faster rate, whereas the observed increase in N_{tot} occurs at a much slower rate, and this causes k_a to decrease.

Overall crystallization kinetics

The developed crystallinity as a function of time at various T_c values from 90 to 65°C and from 60 to 40°C are shown in Figures 7 and 8, respectively. The time to reach complete crystallization, that is, the crystallization time, correlates well with k_a (i.e., the greater k_a is, the shorter the crystallization time is). Consequently, the time to reach complete crystallization decreases with the decrease in T_c from 90 to 65°C, whereas it increases with a further decrease in T_c from 60 to 40°C. The simulated results compare

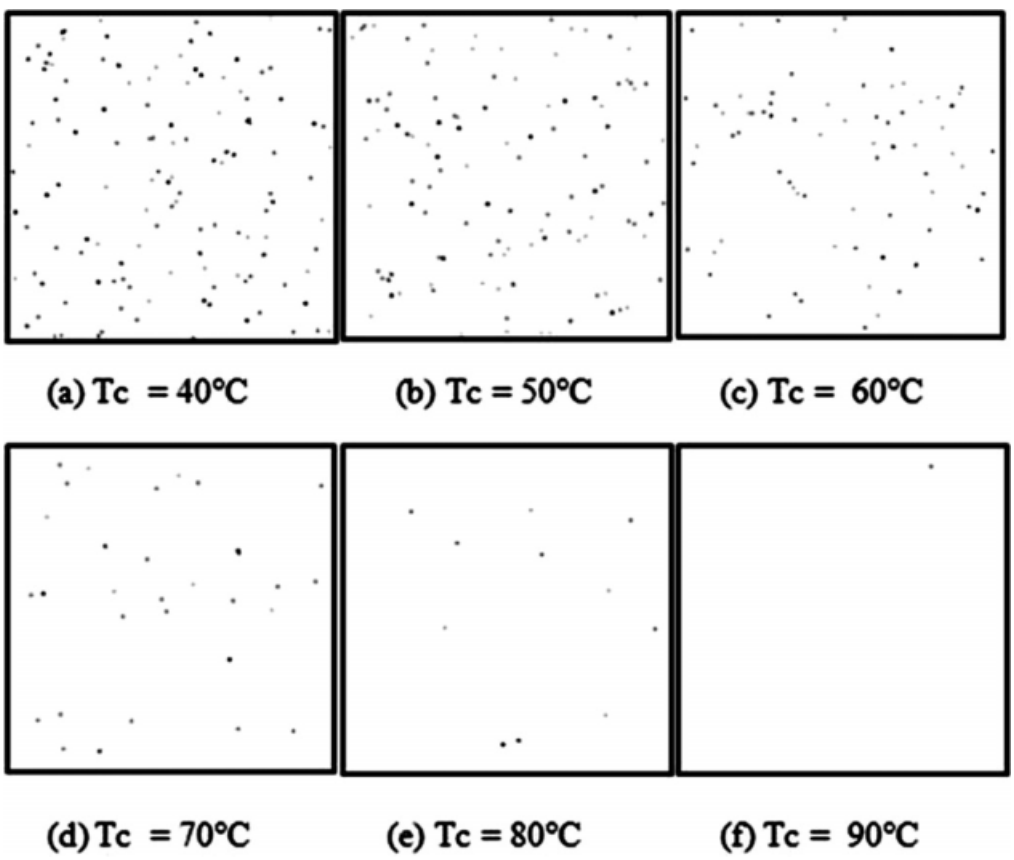

Figure 10 Effect of T_c on N_{tot}: (a) 40, (b) 50, (c) 60, (d) 70, (e) 80, and (f) 90°C.

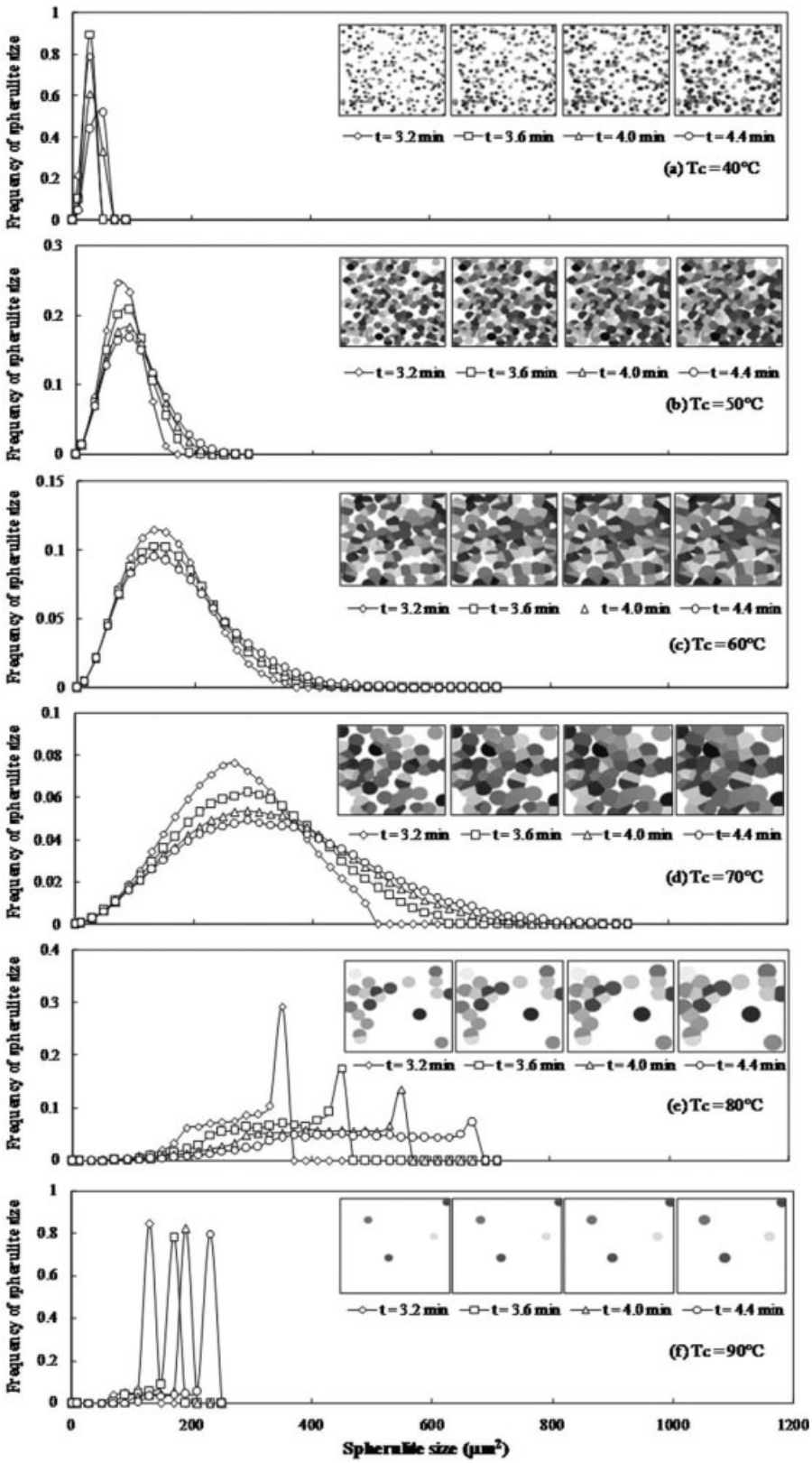

Figure 11 Time evolution of the spherulite size distribution at different T_c values: (a) 40, (b) 50, (c) 60, (d) 70, (e) 80, and (f) 90°C.

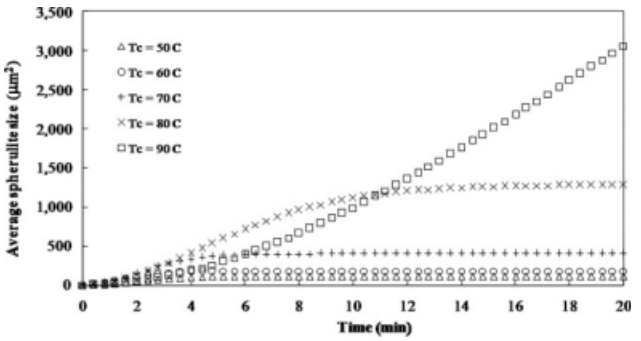

Figure 12 Effect of T_c on the time evolution of the average spherulite size.

well with the experimental results. This clearly confirms the validity of our algorithm. In further validating our model, the developed crystallinity profiles shown in Figures 7 and 8 were analyzed on the basis of the Avrami model, which is based on generalized reduced gradient (GRG2) nonlinear optimization.[19] Figure 9 shows the values of n_a at different T_c values. As expected, the n_a values are close to 2, regardless of T_c. The values near 2 are a result of the assumption made to arrive at the relationship between G and k_a [i.e., eq. (2)].

Morphological development

Figure 10 shows the effect of T_c on N_{tot} during the heterogeneous nucleation process. N_{tot} increases monotonically with decreasing T_c, which is consistent with the results previously shown in Figure 3.

Figure 11 shows the time evolution for the spherulite size distribution during the course of crystallization at various T_c values. The frequency of the spherulite size is calculated from the number of spherulites in a given size range divided by the total number of spherulites. At a given value of T_c, the spherulite sizes, at the beginning of the crystallization process, are relatively small, and the distribution is relatively narrow. During the course of crystallization, the distribution curve shifts to the right-hand side and becomes broader. The result implicates that the majority of the spherulites become larger as they are growing with time, whereas others stop growing as they impinge upon adjacent ones. At the end of the crystallization process, the distribution curve remains unchanged with time (i.e., no more amorphous unit cells are available for further growth).

The effect of T_c on the nucleation mechanism and the transient behavior of the crystallization process can also be inferred from the simulated results shown in Figure 11. At $T_c = 60°C$, the rate at which the amorphous unit cells convert into the crystalline ones is the greatest (see also Fig. 3). At T_c values greater or lower than 60°C, such conversion rates decrease monotonically. Interestingly, the sizes of the majority of the spherulites growing at 80 and especially 90°C are located at the largest end of the distribution curve. This is because, at such high T_c values, N_{tot} is low, and this causes each spherulite to be able to grow independently without impingement. The effect of impingement on the reduction in the sizes of the majority of the spherulites can be observed on the spherulites growing at 80°C.

The effect of T_c on the transient evolution of the average spherulite sizes is emphasized in Figure 12. Clearly, the average size of the spherulites growing at a given value of T_c increases monotonically with the initial increase in the crystallization time and levels off at a certain crystallization time. The critical crystallization time after which constancy in the average spherulite size is observed is related to the extensive impingement of the growing spherulites. At 90°C, the spherulites are able to grow without impinging on adjacent ones, and so we observe a monotonous increase in the average spherulite size with increasing crystallization time (within the range of crystallization times investigated). The effect of T_c on the spherulite sizes at complete crystallization is illustrated in Figure 13. Clearly, the size distribution becomes broader and shifts to the right-hand side with increasing T_c. This indicates that the spherulites get larger with increasing T_c. On the basis of the obtained results, it can be concluded that the final morphology and size of the spherulites are controlled mainly by the number of nuclei (regardless of G), which, in turn, is influenced by the crystallization conditions (e.g., T_c).

CONCLUSIONS

A stochastic simulation accounting for the nucleation and subsequent spherulitic crystal growth under quiescent isothermal crystallization of a semicrystalline polymer was developed. The proposed simulation model was successfully used to describe the effect of T_c on morphological development in detail

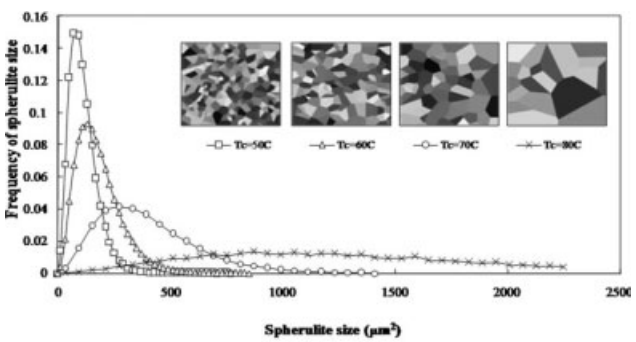

Figure 13 Effect of T_c on the spherulite size distribution at complete crystallization.

during isothermal crystallization of s-PP, which was used as the model polymer. On the basis of previously published experimental data for s-PP, both N_{tot} and G as functions of T_c were obtained. Based on these input data, the conversion of empty unit cells (i.e., the amorphous entity) into occupied ones (i.e., the crystalline entity) during nucleation and subsequent spherulitic crystal growth within a square lattice could be carried out in a systematic manner as a function of T_c. The developed crystallinity, as predicted by this simulation scheme, could also be analyzed by the Avrami macrokinetic model, in which good agreement between the predicted and theoretical values for s-PP was observed. Based on this simulation scheme, both the spherulite size and its distribution during the course of crystallization could also be predicted. It was found that although G influenced both the spherulite size and its distribution during the course of crystallization, it had no effect on the final spherulitic morphology or the resulting average spherulitic size.

References

1. Strobl, G. Prog Polym Sci 2006, 31, 398.
2. Long, Y.; Shanks, R. A.; Stachursili, Z. H. Prog Polym Sci 1995, 20, 651.
3. Schultz, J. M. Polymer Crystallization: The Development of Crystalline Order in Thermoplastic Polymers; American Chemical Society: Washington, DC, 2001.
4. Reiter, G.; Sommer, J.-U. Polymer Crystallization: Observations, Concepts and Interpretations; Springer-Verlag: Berlin, 2003.
5. Capasso, V.; Burger, M.; Micheletti, A.; Salani, C. In Mathematical Modelling for Polymer Processing: Polymerization, Crystallization, Manufacturing; Capasso, V., Ed.; Springer: Berlin, 2003.
6. Huang, T.; Kamal, M. R. Polym Eng Sci 2000, 40, 1796.
7. Priorkowska, E. J Appl Polym Sci 2002, 86, 1351.
8. Lamberti, G.; Titomanlio, G. Eur Polym J 2005, 41, 2055.
9. Raabe, D. Acta Mater 2004, 52, 2653.
10. Raabe, D.; Godara, A. Modell Simul Mater Sci Eng 2005, 13, 733.
11. Xu, H.; Bellehumeur, C. T. J Appl Polym Sci 2006, 102, 5903.
12. Xu, H.; Bellehumeur, C. T. J Appl Polym Sci 2008, 107, 236.
13. Ketdee, S.; Anantawaraskul, S. Chem Eng Commun 2008, 195, 1315.
14. Supaphol, P.; Sprueill, J. E. Polymer 2000, 41, 1205.
15. Supaphol, P.; Sprueill, J. E. Polymer 2001, 42, 699.
16. Avrami, M. J Chem Phys 1939, 7, 1103.
17. Avrami, M. J Chem Phys 1940, 8, 212.
18. Hoffman, J. D.; Davis, G. T.; Lauritzen, J. I., Jr. Treatise on Solid State Chemistry; Plenum: New York, 1976; Vol. 3, Chapter 7.
19. Smith, S.; Lasdon, L. ORSA J Comput 1992, 4, 1.